Conjugation of a brain-penetrant peptide with neurotensin provides antinociceptive properties

Michel Demeule,[1] Nicolas Beaudet,[2] Anthony Régina,[1] Élie Besserer-Offroy,[3] Alexandre Murza,[3] Pascal Tétreault,[2] Karine Belleville,[2] Christian Ché,[1] Alain Larocque,[1] Carine Thiot,[1] Richard Béliveau,[4] Jean-Michel Longpré,[2,3] Éric Marsault,[3] Richard Leduc,[3] Jean E. Lachowicz,[1] Steven L. Gonias,[5] Jean-Paul Castaigne,[1] and Philippe Sarret[2]

[1]Angiochem Inc., Montréal, Quebec, Canada. [2]Department of Physiology and Biophysics and [3]Department of Pharmacology, Faculty of Medicine and Health Sciences and Institut de Pharmacologie, Université de Sherbrooke, Sherbrooke, Quebec, Canada. [4]Laboratoire de Médecine Moléculaire, Université du Québec à Montréal, Montréal, Quebec, Canada. [5]Department of Pathology, UCSD School of Medicine, La Jolla, California, USA.

Neurotensin (NT) has emerged as an important modulator of nociceptive transmission and exerts its biological effects through interactions with 2 distinct GPCRs, NTS1 and NTS2. NT provides strong analgesia when administered directly into the brain; however, the blood-brain barrier (BBB) is a major obstacle for effective delivery of potential analgesics to the brain. To overcome this challenge, we synthesized chemical conjugates that are transported across the BBB via receptor-mediated transcytosis using the brain-penetrant peptide Angiopep-2 (An2), which targets LDL receptor–related protein-1 (LRP1). Using in situ brain perfusion in mice, we found that the compound ANG2002, a conjugate of An2 and NT, was transported at least 10 times more efficiently across the BBB than native NT. In vitro, ANG2002 bound NTS1 and NTS2 receptors and maintained NT-associated biological activity. In rats, i.v. ANG2002 induced a dose-dependent analgesia in the formalin model of persistent pain. At a dose of 0.05 mg/kg, ANG2002 effectively reversed pain behaviors induced by the development of neuropathic and bone cancer pain in animal models. The analgesic properties of ANG2002 demonstrated in this study suggest that this compound is effective for clinical management of persistent and chronic pain and establish the benefits of this technology for the development of neurotherapeutics.

Introduction

Several features of the blood-brain barrier (BBB) prevent diffusion of molecules from the lumen of brain capillaries into surrounding brain tissue. The BBB includes a nonfenestrated capillary endothelium with extensive intercellular tight junctions, multiple intracellular efflux pumps with broad substrate specificity, and an array of intracellular and extracellular enzymes (1, 2). As a result, approximately 98% of systemically administered small molecules, as well as nearly all biologic therapeutic-like recombinant proteins or gene-based medicines, are unable to cross the BBB (3). This restrictive diffusion barrier has been characterized as a major impediment to CNS drug development and is largely responsible for the dearth of pharmacological agents targeting neurological diseases (4, 5).

To overcome the obstacle of drug delivery to the CNS, different strategies have been proposed to increase the transport of therapeutics from blood into brain parenchyma (5, 6). Among the physiological approaches used to improve brain permeability, we have designed a family of peptides, Angiopeps, that bind to a specific receptor expressed on capillary endothelial cells of the BBB (7). Initially characterized as a clearance receptor for chylomicron remnants and α_2-macroglobulin–proteinase (α_2M-proteinase) complexes (8, 9), LDL receptor–related protein-1 (LRP1) is a multiligand receptor with a broad tissue distribution engaged in various biological processes (10). Using both in vitro and in vivo models, we previously demonstrated that upon binding to LRP1 at the luminal membrane of brain capillary endothelial cells, Angiopep-2 (An2) efficiently crosses the BBB by LRP1 receptor-mediated transcytosis (7, 11, 12).
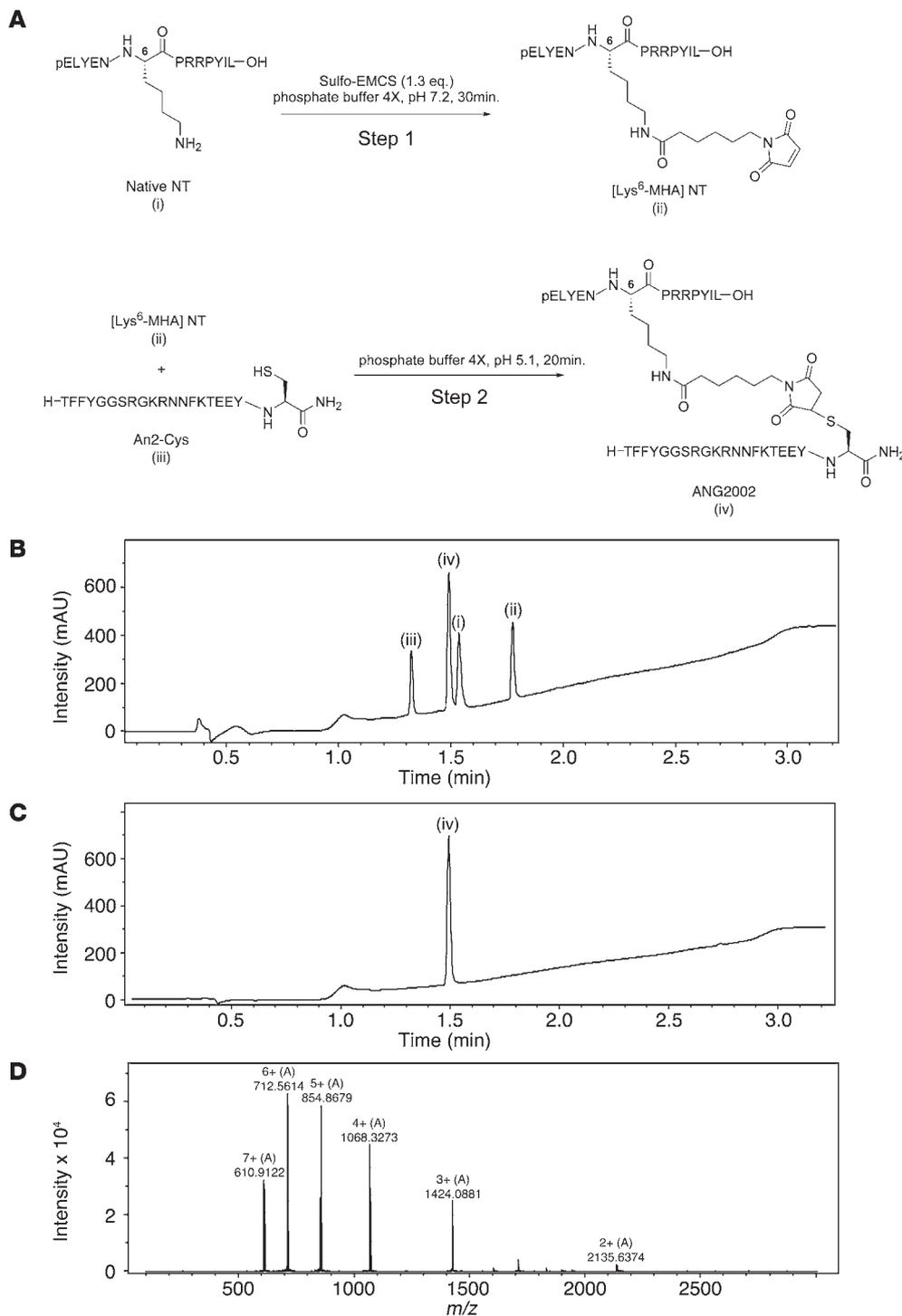
Applying a peptide-drug conjugate strategy, we have created a portfolio of novel anticancer agents, including An2-conjugates of paclitaxel (ANG1005; also known as GRN1005), doxorubicin (ANG1007), and etoposide (ANG1009) (13–16). All 3 of these new molecules have been shown to achieve higher brain penetration than the original unconjugated cancer drugs, while retaining their therapeutic activity. Recently, ANG1005 has demonstrated encouraging preliminary efficacy and safety profiles in phase I/II clinical trials for the treatment of primary and secondary brain tumors (17, 18). Thus, conjugation of An2 to therapeutic drugs having low BBB permeability has proven its efficiency for extending their distribution into brain tissue. The 3 aforementioned anticancer drugs are small molecules of 500–900 Da. BBB penetration of larger molecules, such as therapeutic peptides or proteins, represents the next challenge, for which we established 2 requirements. First, CNS activity of the peptide should be readily measurable to allow for clear demonstration of functional activity. Second, the peptide should be of therapeutic interest if future clinical development is warranted.

technical advance

Figure 1
Synthesis and purification of ANG2002. (**A**) A sulfo-N-[ε-maleimidocaproyloxy]succinimide ester (sulfo-EMCS) linker was attached to the lysine in position 6 of NT and to the C-terminally modified cysteine of An2 to maintain separation of both moieties for functionality purposes. In step 1, 1.3 equivalents of sulfo-EMCS were added to NT. Within 30 minutes, the reaction was acidified and the [Lys[6]-MHA]-NT intermediate purified by HPLC. In step 2, 1.3 equivalents of An2-cysteine were added to the reaction at RT. (**B**) Different retention times were found by analytical RP-UPLC for (i) NT, (ii) [Lys[6]-MHA] NT, (iii) An2-Cys, and (iv) ANG2002. (**C**) Analytical RP-UPLC profile of the purified ANG2002 after the 2-step conjugation reaction. (**D**) Multicharged ESI-TOF MS spectrum of purified ANG2002.

To date, despite substantial investigation, little progress has been made in developing new, effective, and safe analgesics (19). Indeed, most successful analgesic development activity has been confined to the production of congeners and reformulation of existing drugs, or the introduction of drugs initially designed to treat another disease (20). Since the prevalence and burden of chronic pain is large and still growing (21), we decided to apply the An2 strategy to enable brain penetration of the neurotensin (NT) peptide, thereby increasing its analgesic clinical relevance for pain

management. In recent years, the NT tridecapeptide, which exerts biological effects by interacting with 2 distinct GPCRs (termed NTS1 and NTS2), has emerged as an important modulator of nociceptive transmission (22–25). Existing data also indicate that the analgesic effects of NT are independent of the endogenous opioid system (26–30), and may act synergistically with opioids to reduce pain (31–33). In the present study, we investigated whether a novel An2-NT conjugate, ANG2002, can access brain parenchyma after systemic administration while retaining the analgesic properties
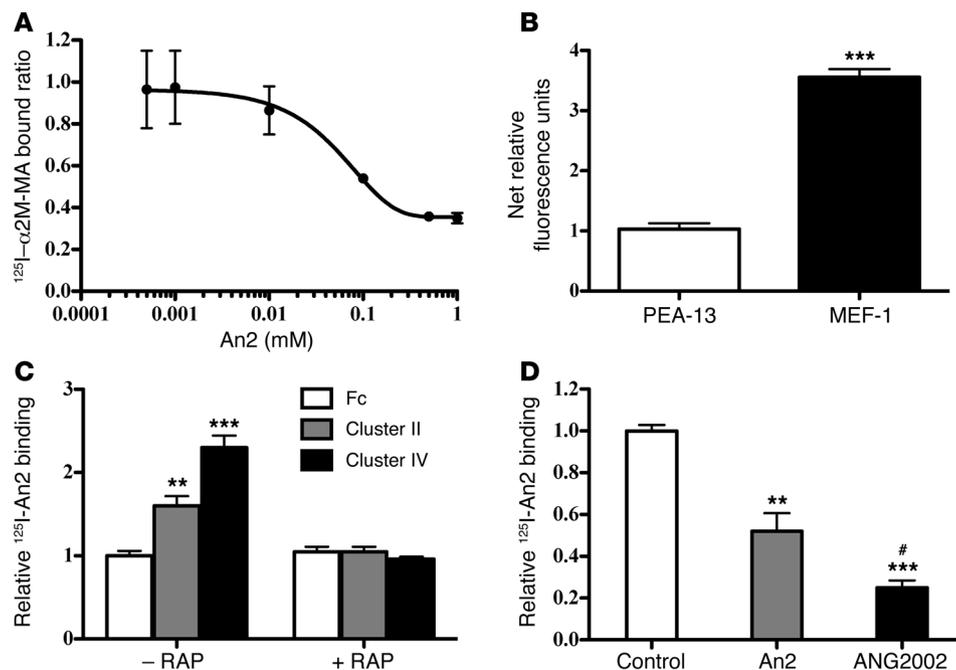
Figure 2
Molecular interaction of An2 and ANG2002 with LRP1. (**A**) An2 inhibition of specific α_2M-MA binding to LRP1 on MEF cells. Cells were incubated with 0.1 nM α_2M-MA in the presence or absence of increasing concentrations of An2. (**B**) Uptake of Alexa Fluor 488–labeled An2 in LRP1-positive MEF-1 fibroblasts and LRP1-deficient PEA-13 fibroblasts. (**C**) Binding of ^{125}I-An2 to Fc, CCR-2 (Cluster II), and CCR-4 (Cluster IV) with and without preincubation with 0.5 μM RAP. (**D**) Binding of ^{125}I-An2 to CCR-4 performed in the absence and presence of excess unlabeled An2 or ANG2002 (500 μM). Data represent mean ± SD. **$P < 0.01$, ***$P < 0.001$ versus respective control; #$P < 0.05$ versus An2; Student's t test (**B**), 2-way ANOVA followed by Bonferroni post-test (**C**), or 1-way ANOVA followed by Bonferroni correction (**D**).

of the native NT peptide in animal models of nociception. Our results indicate that An2-NT may represent a novel therapeutic candidate for persistent and chronic pain.

Results

Synthesis and purification of ANG2002
ANG2002 was synthesized by a 2-step conjugation of the tridecapeptide NT to the 19–amino acid LRP1-binding peptide An2 (Figure 1A). Reverse-phase ultra-performance liquid chromatography (RP-UPLC) analysis demonstrated that ANG2002 and its precursors showed different retention times (Figure 1B). ANG2002, which was purified by HPLC, had a final yield of 48% and purity greater than 95% (Figure 1C). Multicharged ESI-TOF mass spectrometry (MS) yielded a mass of 4,269.11 Da, in good agreement with the predicted mass of ANG2002 (4,269.75 Da, $C_{195}H_{287}N_{53}O_{54}S$; Figure 1D).

Transport of An2 and ANG2002 across the BBB
We previously reported that LRP1 is involved in transport of An2 across the BBB (11, 12). To study the binding of ANG2002 to LRP1, we examined the ability of the conjugate to compete with radioiodinated methylamine-activated α_2M (α_2M-MA) for binding to LRP1-expressing MEF-1 cells. In these cells, LRP1 is the exclusive high-affinity receptor for α_2M-MA (34). As shown in Figure 2A, An2 competitively inhibited binding of ^{125}I-labeled α_2M-MA to LRP1-expressing MEF-1 cells in a dose-dependent manner. At the highest concentration, An2 did not fully displace α_2M-MA binding to LRP1-expressing MEF-1 cells. This result may reflect the fact that α_2M-MA recognizes different binding cluster regions than other LRP1 ligands, notably the first cluster of complement-like repeats (35). Endocytosis of An2 was studied using a fluorescently labeled derivative. In these studies, MEF-1 cells showed a 3.4-fold increase in Alexa Fluor 488–labeled An2 compared with LRP1-deficient PEA-13 cells (Figure 2B). These results suggest that LRP1 is mostly responsible for the endocytosis of An2.

To examine the binding of An2 and ANG2002 to LRP1 in a purified system, we expressed the clusters of complement-like repeats in LRP1, which are responsible for the majority of LRP1-ligand interactions, as Fc fusion proteins (36–38). Fc-LRP1 clusters II and IV (CCR-2 and CCR-4, respectively) both demonstrated increased binding of ^{125}I-labeled An2 compared with free Fc, with preferential binding for CCR-4 (Figure 2C). To confirm the specificity of the interaction, binding studies were repeated in the presence of the LRP1 antagonist receptor-associated protein (RAP). The increase in binding of ^{125}I-labeled An2 to CCR-2 and CCR-4 was entirely blocked by RAP, which demonstrated that, like most other LRP1 ligands, An2 bound to both LRP1 clusters by a RAP-inhibitory mechanism. To determine whether ANG2002 also binds to LRP1, we compared the ability of unlabeled ANG2002 and An2 to displace ^{125}I-labeled An2 from CCR-4. ANG2002 was at least as effective as An2 as a competitor for CCR-4 binding (Figure 2D).

In vitro functionality of ANG2002 on NT receptor signaling
We next determined whether ANG2002 conserved the biological activity of the NT native peptide (Table 1). Competitive binding studies revealed that the calculated IC$_{50}$ for ANG2002 (13.0 nM; 95% CI, 11.6–14.5) was similar to that of the endogenous NT peptide on CHO-K1 cells stably expressing human NTS1 (14.8 nM; 95% CI, 13.6–16.0). Likewise, ANG2002 binding to 1321N1 cells stably expressing human NTS2 (3.3 nM; 95% CI, 2.8–4.0) also approximated that of NT (6.2 nM; 95% CI, 5.2–7.5). Thus, the An2 moiety did not affect the NT receptor binding affinity. We then examined whether ANG2002 was still able to induce β-arrestin recruitment and G protein activation through NTS1 or NTS2 stimulation. Bioluminescence resonance energy transfer (BRET) assays revealed that ANG2002 and NT were equally effective in recruiting β-arrestin2 after activation of NTS1 (Table 1). Our results also showed that the G protein functional coupling was not impaired by conjugation of the An2 peptide. Indeed, we found that ANG2002 conserved its capacity to activate the G proteins

technical advance

Table 1

Cell-based functional assays used to characterize ANG2002 versus native NT signaling activity at the NTS1 receptor site

GPCR coupling	NT	ANG2002
β-arrestins	10.11 (6.42–15.91)	13.83 (9.49–20.16)
G_q	0.34 (0.18–0.64)	2.04 (1.55–2.70)
G_{oA}	2.93 (2.17–3.96)	5.95 (4.21–8.42)
G_{13}	35.47 (28.32–44.43)	33.76 (19.24–59.23)

Data represent EC_{50} (nM) and 95% CI.

G_q, G_{oA}, and G_{13} through binding to NTS1 (Table 1). Likewise, in 1321N1 cells stably expressing human NTS2, both ANG2002 and NT produced a rapid and sustained increase in ERK1/2 phosphorylation (Supplemental Figure 1; supplemental material available online with this article; doi:10.1172/JCI70647DS1), indicative of functional coupling to NTS2 receptors.

In vivo brain penetration and plasma stability of ANG2002

Once the in vitro functionality of both An2 NT peptide moieties in ANG2002 was verified, we examined whether ANG2002 could effectively cross the BBB. Using an adapted in situ brain perfusion method (7, 12), we determined the penetration time courses of [125I]-NT and [125I]-ANG2002 into the CNS after peripheral (intracarotid) administration. After brain perfusion, a time-dependent linear increase in the distribution volume (V_d) of [125I]-ANG2002 was observed (Figure 3A). The V_d of ANG2002 in total brain homogenate after 4 minutes of perfusion was 62.4 ± 0.7 ml/100 g brain, significantly greater than that of the NT native peptide (7.4 ± 1.4 ml/100 g), providing in vivo evidence in support of ANG2002 penetration into the brain. Accordingly, the slopes of the line, corresponding to the BBB influx rate constant (K_{in}), was 10-fold greater for ANG2002 (2.7×10^{-3} ml/s/g) than for unconjugated NT (2.7×10^{-4} ml/s/g). As expected, [14C]-inulin control in the presence of ANG2002 was unable to penetrate brain tissue (data not shown), which confirmed the physical integrity of the BBB in these experiments.

To test whether ANG2002 entered brain parenchyma or remained associated with the brain capillary endothelium, we estimated the apparent V_d for ANG2002 and NT in total brain tissue, capillaries, and parenchyma after in situ perfusion and brain capillary depletion. At 2 minutes after administration, ANG2002 had a higher V_d than unconjugated NT not only in total brain tissue, but also in isolated brain parenchyma (Figure 3B). Indeed, approximately 70% of [125I]-ANG2002 was associated with the parenchymal fraction, which indicated that a substantial proportion of ANG2002 crossed the BBB, rather than remaining bound to or trapped within the vasculature endothelium. Higher V_d values for ANG2002 relative

Figure 3

Brain uptake of ANG2002 and NT measured by in situ mouse brain perfusion. (**A**) Time course of brain uptake of [125I]-ANG2002 and [125I]-NT. Results represent apparent V_d in total brain homogenate. Lines represent best fits to the data by least-squares regression. (**B**) After a 2-minute perfusion of [125I]-ANG2002 (black bars) and [125I]-NT (white bars), brain capillary depletion was performed, and radioactivity was quantified in total brain homogenate, brain capillary fractions, and brain parenchymal fractions. Results represent apparent V_d for the radiolabeled drugs in the indicated compartments. Data represent mean ± SD (n = 4–6 mice per time point). *P < 0.05, **P < 0.01 vs. NT, Student's t test.

to NT were also observed in the capillary fraction (Figure 3B), consistent with higher passage rate through the BBB.

We further evaluated whether ANG2002 was present in its intact form in brain tissue after brain perfusion (Supplemental Figure 2). HPLC analyses revealed that after intracarotid administration, 80% of the radioactivity was associated with ANG2002 elution fractions, which indicated that high levels of intact ANG2002 crossed the BBB and reached the brain parenchyma.

In a second set of experiments, we determined the stability and the degradation profile of the NT moiety of ANG2002 in plasma, compared with the native NT peptide. The degradation kinetics of NT and ANG2002 were assessed by HPLC-MS analyses after incubation for up to 7 hours at 37°C with either rat or mouse plasma. Incubation of native NT with rat or mouse plasma resulted in rapid and complete degradation of the NT peptide, the cleavage occurring at the dibasic Arg8-Arg9 residues (Supplemental Table 1). While native NT degraded in less than 30 minutes, no cleavage products of the NT moiety of the ANG2002 conjugate were identified before 7 hours in rat plasma, which suggests that An2 protects the NT moiety from the proteolysis. Interestingly, marked species differences were also observed in the plasma stability profiles of ANG2002. The NT moiety of ANG2002 was stable for less than 1 hour in mouse plasma. Therefore, ANG2002 remained intact for a longer period of time in rat plasma than in mouse plasma, perhaps contributing to the higher analgesic potency observed in rats versus mice.

Analgesic potency of ANG2002 in different experimental pain models

Acute pain models. We first used 2 acute pain models (hot-plate and tail-flick assays) to test whether i.v. delivery of ANG2002 attenuates the withdrawal responses to thermal nociceptive stimuli
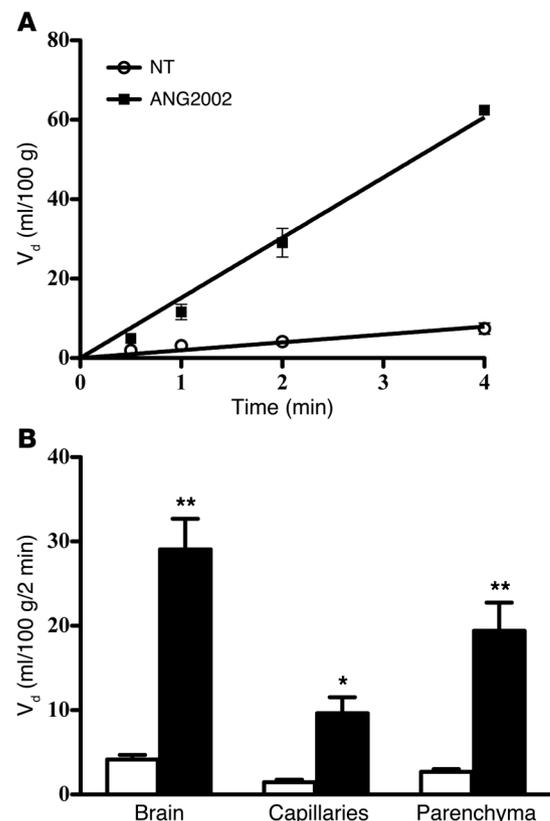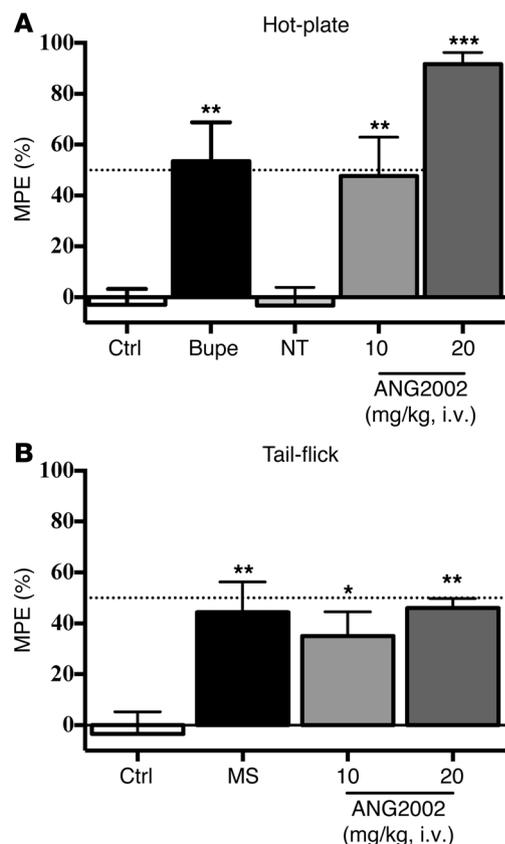
Figure 4
Antinociceptive responses to ANG2002 in acute pain models. (**A**) Hot-plate test performed on CD-1 mice after administration of ANG2002 (10 and 20 mg/kg i.v.), NT (8 mg/kg i.v.), or buprenorphine (Bupe; 1 mg/kg s.c.). (**B**) Analgesic effects of ANG2002 and morphine sulfate (MS; 5 mg/kg i.p.), assessed by mouse radiant heat tail-flick assay. MPE was calculated at the time of peak antinociceptive response. *$P < 0.05$, **$P < 0.01$, ***$P < 0.001$ versus saline control, 1-way ANOVA followed by Dunnett multiple comparison test.

ly, coadministration of the antagonist SR142948A inhibited both NT- and ANG2002-induced increases in tail withdrawal latency (Figure 5A). These results demonstrated that the analgesic effects of ANG2002 were produced by agonist activity at NT receptors.

To further define the respective roles of NTS1 and NTS2 receptors in ANG2002-induced analgesia, both NTS1- and NTS2-knockout C57BL/6 mice were subjected to the tail-flick test after i.v. administration of ANG2002 (5 mg/kg). As previously observed (30, 41), the baseline pain thresholds in both genotypes were not significantly different from thresholds in WT littermates. Injection of ANG2002 i.v. induced potent analgesic responses in NTS1- and NTS2-deficient mice (Figure 5, B and C), which suggests that ANG2002 exerts its antinociceptive action by acting at both NTS1 and NTS2 sites.
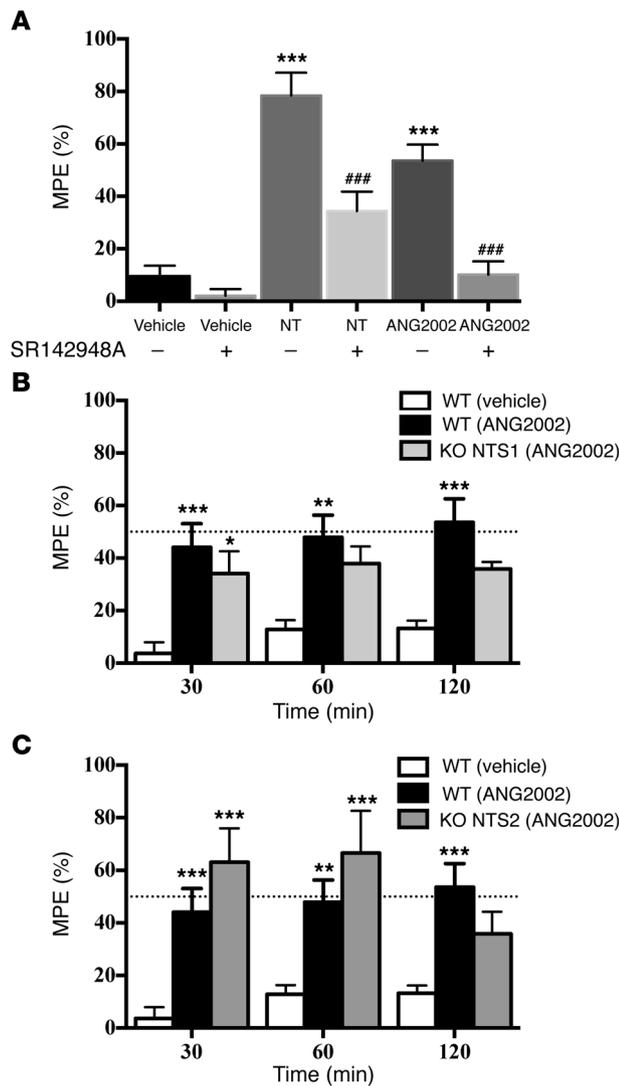
Formalin tonic pain model. Intraplantar injection of formalin into the right hind paw of saline-treated rats produced a typical biphasic nociceptive behavioral response, consisting of an acute phase (phase I; 0–9 minutes) followed by a prolonged inflammatory phase (phase II; 21–60 minutes) (Figure 6). Administration of ANG2002 i.v. induced a dose-dependent antinociceptive effect in both phases of the formalin model of persistent pain, characterized by a decrease in the weighted pain score compared with saline values (Figure 6A). The ED_{50} of ANG2002 was 0.009 and 0.016 mg/kg for phases I and II, respectively (Figure 6, C and D). Notably, i.v. morphine did not produce any antinociceptive response at the effective analgesic dose found for ANG2002 (0.05 mg/kg). The An2 peptide (5 mg/kg) had no influence on formalin-induced pain behaviors by itself (Figure 6B).

Pain intensity elicited by formalin administration may also be rated by monitoring the total time spent in different behavioral endpoints (i.e., lifting, flinching, licking, biting) (42). It was notably demonstrated that these stereotypical nociceptive reactions are integrated at different levels of the pain neuraxis (43). Consistent with the weighted-scores method, we found that ANG2002 markedly and dose-dependently decreased the formalin-induced flinching, licking, and biting responses in both phase I and phase II (Figure 6, E and F), which indicates that ANG2002 affects supraspinally processed pain-related behaviors. Conversely, morphine and An2 were not effective in reversing these spontaneous aversive behaviors (Figure 6G).

Neuropathic pain model. We next investigated whether ANG2002 can attenuate neuropathic pain behaviors induced by chronic constriction injury (CCI) of the sciatic nerve. Hypersensitivity to mechanical stimuli was examined in sham- and CCI-operated rats during the 3-week period after surgery (Figure 7A). The paw withdrawal threshold (PWT) in response to innocuous tactile stimuli significantly decreased on the ipsilateral hind paw 7 days after surgery and persisted for at least 21 days compared with presurgery baseline values ($23.5 ± 1.4$ g vs. $43.7 ± 0.8$ g; $P < 0.001$). Sham-operated rats did not develop mechanical allodynia throughout the 3-week testing period (Figure 7A). Punctual i.v. delivery of

(Figure 4). Male CD-1 mice placed on a heated surface (54°C) did not exhibit any difference in the latency of foot-licking response between experimental groups at baseline. For all tested drugs, peak antinociception consistently occurred 15–30 minutes after injection. At the peak of response, ANG2002 caused significant increases in hot-plate latency, producing approximately 90% of the maximum possible effect (MPE) at the highest dose ($P < 0.001$ vs. control; Figure 4A). In the same experimental pain model, mice receiving buprenorphine (1 mg/kg s.c.) also exhibited an increase in their reaction times (~55% MPE; $P < 0.01$ vs. control; Figure 4A). Importantly, i.v. administration of an equimolar dose of the non-brain-penetrant native NT was ineffective in reducing the nociceptive behaviors to noxious thermal stimulation.

The heat radiant tail-flick test was also used to assess the analgesic effects of ANG2002 (Figure 4B). Comparison of MPE at 30 minutes after injection showed significant effects for every dose, with the highest dose inducing maximal elevation of the tail-flick threshold (~46% MPE; $P < 0.01$; Figure 4B). CD-1 mice acutely treated with morphine (5 mg/kg i.p.) also showed decreased sensitivity to heat stimulation (~44% MPE; $P < 0.01$; Figure 4B).

To ensure that the neurotensinergic system was involved in ANG2002-induced analgesia, we next examined using the tail-immersion test whether the NTS1/NTS2-selective nonpeptide antagonist SR142948A (39) could block the analgesic effects of ANG2002. To allow for direct comparison, both NT and ANG2002 were administered intrathecally (i.t.), since i.v. NT does not induce analgesia because of its poor BBB penetration. As previously reported (40), NT increased the nociceptive threshold in the tail-flick test (Figure 5A). Likewise, i.t. injection of an equimolar dose of ANG2002 produced a similar analgesic response. More important-

technical advance

A

B

C

Figure 5
Effect of NT receptor inactivation on ANG2002-induced analgesia. (**A**) Influence of the NT receptor antagonist SR142948A on NT- and ANG2002-induced antinociceptive responses. MPE was calculated 60 minutes after i.t. injection. In the presence of 10 μg/kg SR142948A, antinociceptive responses to NT (20 μg/kg) and ANG2002 (50 μg/kg) were significantly reduced. No change in tail-flick latencies was seen after administration of SR142948A alone. ***$P < 0.001$ versus saline vehicle; ###$P < 0.01$ versus no SR142948A; 1-way ANOVA followed by Bonferroni post-test. (**B** and **C**) WT, NTS1-deficient (**B**), and NTS2-deficient (**C**) C57BL/6 mice submitted to the tail-immersion test after i.v injection of ANG2002 (5 mg/kg). In both NTS1-deficient and NTS2-deficient mice, ANG2002 conserved its analgesic properties. *$P < 0.05$, **$P < 0.01$, ***$P < 0.001$ versus vehicle-treated WT, 2-way ANOVA followed by Bonferroni post-test.

Measurement of physiological variables
Besides its prominent antinociceptive action, the NT peptide was also reported to modulate blood pressure and body temperature (46, 47). We therefore measured time courses of mean arterial blood pressure (MAP) and core body temperature before and after treatment with various doses of ANG2002 (Figure 8). After i.v. bolus delivery, ANG2002 dose-dependently produced a drop in blood pressure (Figure 8A). This blood pressure reduction (50–60 mmHg at the larger dose) persisted for 15–20 minutes after drug administration. Similarly, NT (2 mg/kg i.v.) provoked a drop in MAP (Figure 8A). Variations in body temperature, determined as change from baseline, were also recorded over 6 hours after ANG2002 injection. Our results demonstrated that 5 mg/kg ANG2002 induced long-term hypothermia up to 4 hours after administration (Figure 8B). Importantly, at the dose of 0.05 mg/kg, which was shown to exert analgesic actions, ANG2002 did not induce either hypothermia or blood pressure drops.

We finally verified whether the analgesic efficacy of the 0.05-mg/kg ANG2002 dose could potentially be confounded by locomotor-depressant side effects. ANG2002-treated rats were submitted, at a time corresponding to the analgesic peak (30–45 minutes), to behavioral tasks assessing locomotor and exploratory activities as well as motor coordination. The open-field activity test used to characterize exploratory behaviors — such as total distance traveled, time of immobility, and movement pattern — showed no overall difference between vehicle- and ANG2002-treated rats (Figure 8C). Likewise, the Rotarod, used in the acceleration mode (from 4 to 40 rpm), revealed that ANG2002 did not affect motor performance (i.e., time spent on the rod) (Figure 8D).

Discussion
In the current study, we conjugated NT, an endogenous tridecapeptide with recognized analgesic properties (22–25), to An2, a proprietary 19–amino acid peptide that crosses the BBB by receptor-mediated transcytosis (7, 12). The primary goal of this research was to assess whether the An2-based platform, which has proven to be effective with small-molecule anticancer agents in the past (13–18), could be extended to larger peptide therapeutics. Validation of this approach required 4 criteria to be met: first, that the An2-NT conjugate retains its binding to the BBB LRP1 receptor; second, that the conjugation does not interfere with the binding and pharmacological activity of the native NT peptide; third, that the new molecular entity penetrates the BBB efficiently after systemic administration; and fourth, that it induces biologic responses similar to centrally administered NT. All of these requirements were fulfilled in the present study.

ANG2002 at the dose found to be effective in the formalin pain model (i.e., 0.05 mg/kg) successfully attenuated ongoing tactile allodynia, achieving 52% of pain relief 45 minutes after drug injection (Figure 7A). With respect to the antiallodynic effect, ANG2002 induced sustained analgesia over the 2-hour period (Figure 7B).

Bone cancer pain model. Finally, we validated the effect of ANG2002 on bone cancer pain. This model of mixed pain involving neuropathic and inflammatory components is one of the most severe and intractable types of chronic pain reported (44, 45). Cancer-bearing rats inoculated with 30,000 MRMT-1 cells directly into the femur displayed a decreased PWT in the dynamic von Frey test compared with sham-operated animals (Figure 7C). As previously observed (44, 45), tactile allodynia progressively developed until day 18, reaching a 60% decrease of the mechanical threshold (17.2 ± 1.2 g vs. 42.6 ± 1.0 g; $P < 0.001$). After pain detection on day 18, we evaluated the effects of i.v. ANG2002 administration on mechanical hypersensitivity induced by tumor progression. Our results demonstrated that 0.05 mg/kg ANG2002 induced a significant 43% PWT recovery compared with the vehicle-treated group 45 minutes after drug delivery (Figure 7C). This partial reversal of the allodynic state was maintained over the 2-hour period (Figure 7D).
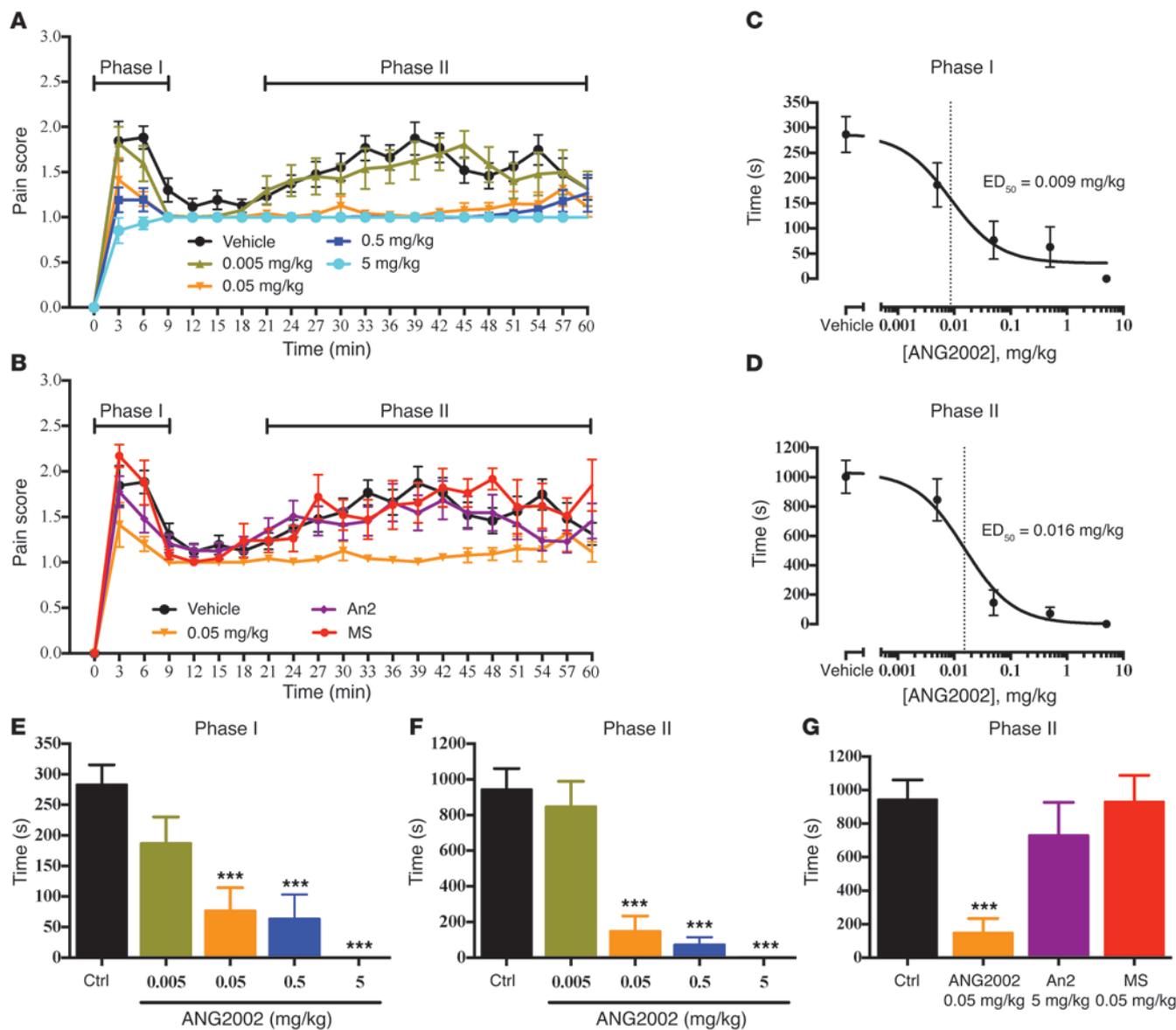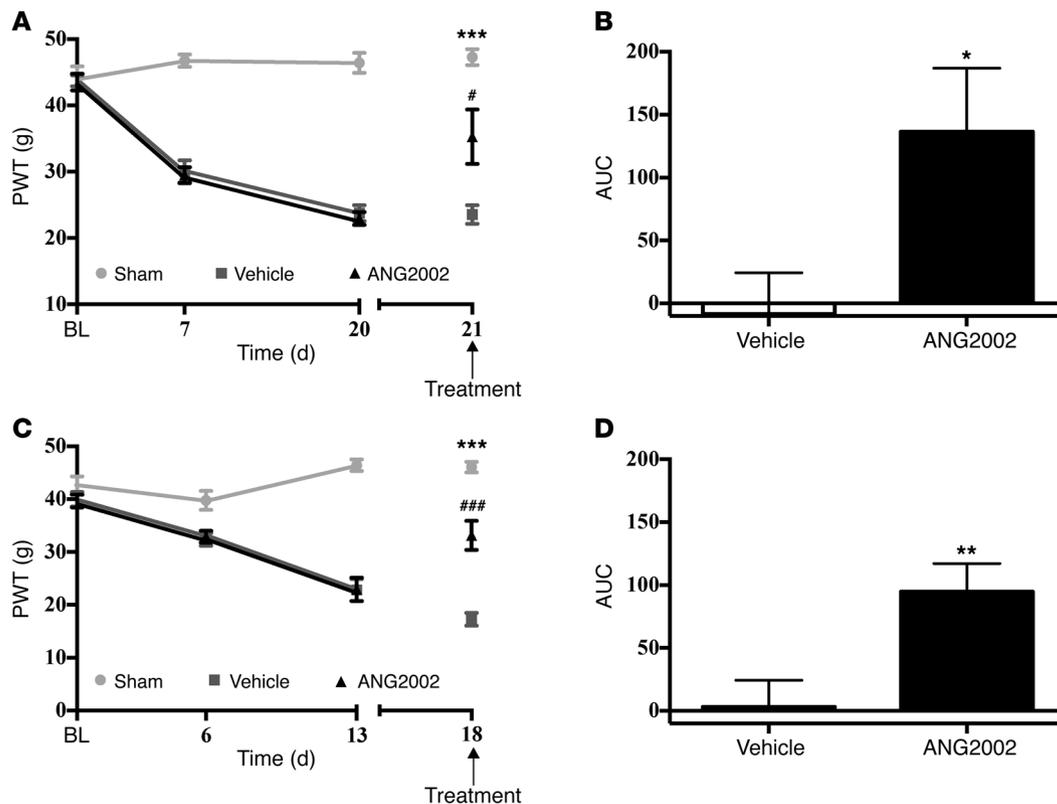
Figure 6
Analgesic efficacy of ANG2002 in the formalin model of tonic nociceptive pain. (**A**) ANG2002 dose-response analgesic effect on reducing formalin-induced nociceptive pain behaviors after i.v. administration. (**B**) Analgesic effect of i.v. morphine sulfate (0.05 mg/kg) compared with ANG2002 (0.05 mg/kg) and An2 (5 mg/kg). (**C** and **D**) ANG2002 ED_{50} in acute (0–9 minutes; **C**) and inflammatory (21–60 minutes; **D**) phases. (**E**) Effect of ANG2002 on time spent flinching, licking, and biting in the acute phase of the formalin test. (**F** and **G**) Time spent flinching, licking, and biting in the inflammatory phase of the formalin test. n = 6–10 rats per group. ***$P < 0.001$ versus control, 1-way ANOVA followed by Dunnett multiple-comparison test (**E** and **F**) or Kruskal-Wallis test followed by Dunn correction (**G**).

The BBB tightly regulates the movements of nutrients and metabolites between the blood and the CNS to maintain cerebral homeostasis. In addition, the BBB protects the brain from injuries and diseases by limiting the entry of circulating pathogens or toxic agents (1). Paradoxically, this natural defense is also the most significant obstacle to effectively treat many CNS disorders; existing drugs have limited ability to penetrate the brain at therapeutic concentrations after systemic administration (4, 48). Indeed, almost all large molecules, including peptides, enzymes, monoclonal antibodies, recombinant proteins, and gene-based therapies, do not cross the BBB (5, 6).

Neuropeptides play a crucial role in regulation of the brain, and peptide receptors hold great promise in advancing structure-based drug discovery for the treatment of CNS disorders (49). Thereby, several strategies have been developed over the last 2 decades to overcome the physicochemical limitations of these endogenous peptides. Notably, successful approaches have been applied to increase their chemical stability and reduce their rapid clearance and enzymatic degradation. However, one of the major remaining challenges in the development of peptides as potential drugs is to achieve optimal CNS concentrations. Different approaches have been tested to bypass the BBB, including transcranial or i.t. drug delivery, disrup-
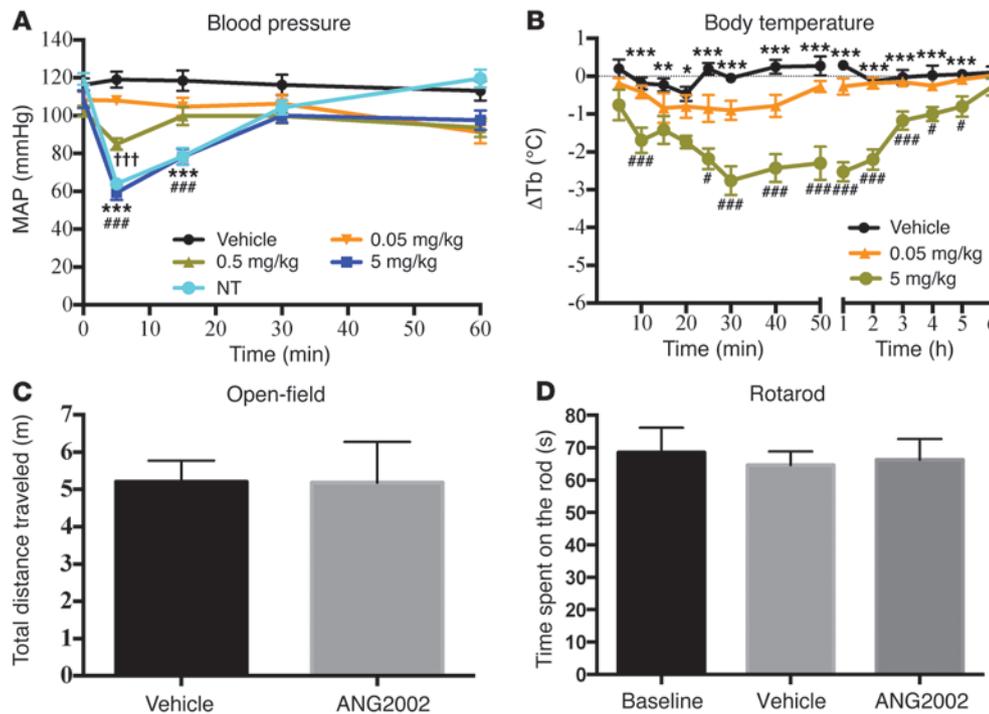
Figure 7
Antiallodynic effects of ANG2002 in 2 chronic pain models. (**A**) Effect of ANG2002 on tactile allodynia induced by CCI of the sciatic nerve. PWT after automated von Frey hair stimulation was measured at various time points after induction of neuropathic pain. On day 21, rats were given i.v. administration of ANG2002 (0.05 mg/kg) or vehicle. The antiallodynic effect was evaluated 45 minutes after administration. BL, baseline. (**B**) The antiallodynic effect was monitored at additional time points (75 and 120 minutes) after ANG2002 injection and calculated as AUC over the 2-hour period. (**C**) Effect of ANG2002 on mechanical allodynia induced by the inoculation of the syngeneic mammary tumor cell line MRMT-1 into the femoral bone. The time course of tactile allodynia was examined in cancer-bearing and sham-operated rats during the 3-week period after the surgery. PWT was determined at day 18, 45 minutes after acute i.v. injection of either ANG2002 (0.05 mg/kg) or vehicle. (**D**) The effect of ANG2002 was monitored at additional time points (75 and 120 minutes) after ANG2002 injection and calculated as AUC over the 2-hour period. n = 8–10 rats per group. (**A** and **C**) ***$P < 0.01$, ###$P < 0.001$ versus vehicle, 1-way ANOVA followed by Dunnett multiple comparison test. (**B** and **D**) *$P < 0.05$, **$P < 0.01$, Student's unpaired t test.

tion of the BBB by osmotic shock, and drug nanoparticle formulations (5, 50). However, these approaches are either ineffective in reaching the brain parenchyma, invasive, or limited to inducing drug distribution into the brain by passive diffusion. In recent years, considerable effort has been made to implement new techniques that direct neuropharmaceutical agents across the BBB (50, 51). These technologies take advantage of the presence of endogenous receptors or transporters highly expressed at the BBB interface to facilitate drug-brain uptake. Thus, ligands and monoclonal antibodies to these carriers can be used as Trojan horses for active transcytosis of peptide pharmaceuticals to the brain.

We opted for a strategy using the Angiopep/LRP1 complex to circumvent the BBB restriction. We showed that ANG2002 displaced [125I]-An2 binding to CCR-4 at least as effectively as An2, demonstrating that the LRP1-binding property of An2 was preserved upon conjugation with NT. We also showed that ANG2002 bound to NTS1 and NTS2 receptors in the low nanomolar range, thus exhibiting a similar binding affinity to that of native NT. We further found that ANG2002 and NT were equally effective in inducing β-arrestin2 recruitment, G protein functional coupling, and second

signaling pathway activation after stimulation of NTS1 or NTS2. To address the third criterion, we evaluated brain uptake of [125I]-ANG2002 using in situ mouse brain perfusion. [125I]-ANG2002 exhibited a 10-fold augmentation of K_{in} compared with native NT. Capillary depletion experiments further demonstrated that approximately 70% of the tracer was associated with the parenchymal fraction; that is, a significant proportion of ANG2002 appeared to fully translocate across the BBB, rather than remain bound to the vascular endothelium. Importantly, we also found that in contrast to the rapid cleavage of the native NT peptide in rat plasma, the NT moiety of ANG2002 was proteolytically stable for up to 7 hours, and the majority of ANG2002 was present in its intact form in brain tissue after i.v. administration. In addition, the analgesic activities of systemically administered ANG2002 in models of nociception were very similar to those of centrally administered NT (22–25). Finally, the hypotensive and hypothermogenic responses, which were previously reported for the NT peptide (46, 47), were not observed with the low analgesic dose of ANG2002. Thus, ours is the first demonstration of active transport of a neuropeptide using a family of peptides targeting an endogenous receptor system within the BBB.

Figure 8
Effects of ANG2002 on physiological parameters. (**A**) MAP was determined for 60 minutes after i.v. administration of ANG2002 (0.05, 0.5, or 5 mg/kg) or NT (2 mg/kg) in Wistar male rats. ***$P < 0.001$, NT vs. vehicle; ###$P < 0.001$, 5 mg/kg ANG2002 vs. vehicle; †††$P < 0.001$, 0.5 mg/kg ANG2002 vs. vehicle; 2-way ANOVA followed by Bonferroni post-test. (**B**) Change in body temperature (ΔTb) over a 6-hour time span after i.v. ANG2002 injection in Sprague-Dawley rats. *$P < 0.05$, **$P < 0.01$, ***$P < 0.001$ versus 5 mg/kg ANG2002; #$P < 0.05$, ###$P < 0.001$ versus 0.05 mg/kg ANG2002; 2-way ANOVA followed by Bonferroni multiple comparison test. (**C**) Spontaneous locomotor activity assessed using the open field. Rats treated with ANG2002 (0.05 mg/kg) traveled total distances similar to those of saline-treated animals (unpaired t test). (**D**) Motor balance and coordination were evaluated using the Rotarod test after ANG2002 (0.05 mg/kg) treatment. The time the animal spent on the Rotarod (e.g., latency to fall) was measured (1-way ANOVA followed by Bonferroni post-test).

effects reported in the use of chronic opioid medications (22–25). However, the approach described in this work substantially differs from other approaches taken in the past for NT therapeutics, most notably those that explored the utility of chemically modifying NT fragments (typically consisting of the 6 C-terminal amino acids of the peptide) as a means of allowing systemic administration. Most of these compounds are highly modified versions of NT_{8-13}, with substitutions, reduced peptide bonds, cyclization, and/or other structural changes that increase stability of the molecule in the blood. The first BBB-crossing NT_{8-13} analog with antinociceptive properties, NT1 (also referred to as the Eisai hexapeptide), was modified at amino acid residues 8, 9, 11, and 12. Specifically, N-methyl-Arg, Lys, Trp, and tert-Leu were substituted for Arg, Arg, Tyr, and Ile, respectively (60–64). Likewise, PD149163, a reduced-amide NT_{8-13}, showed improved metabolic stability after systemic administration and maintained the analgesic activities of the native NT peptide

A detailed analysis of ANG2002 neuroanatomical localization after penetration of the BBB remains to be documented, but the observed antinociceptive activities provide strong evidence that the molecule crosses the BBB to reach brain structures involved in descending sensory inhibition, such as the periaqueductal grey and the rostral ventromedial medulla, which are known to express high levels of NT receptors (52–56). The potentially broad parenchymal distribution of ANG2002 was also observed for other An2 conjugates (12–16) or kunitz-derived peptides (7), likely reflecting the extraordinarily high density of cerebral capillaries (57) as well as the broad distribution of LRP1 throughout the brain-capillary tree (58, 59). Accordingly, we demonstrated using a Cy5-labeled An2 peptide that An2 was transported very efficiently in rat brain parenchyma, as measured by in vivo imaging followed by fluorescence analysis of brain sections (11). Development of an ANG2002 radiopharmaceutical for PET will further assist in visualizing its spatial and temporal brain distribution in live animals.

We chose the An2-NT conjugate as our preliminary test molecule because of its intrinsic analgesic potential at the CNS level. Indeed, we and others have demonstrated that the transmission of pain information is strongly influenced by the activity of the neurotensinergic system and that NTS1/NTS2 agonists may represent a new class of potent analgesics without the side

(65–67). Subsequently, several additional systemically infused but centrally acting analogs (i.e., NT66L, NT69L, NT79, and ABS212) were synthesized by combining N-terminal modifications and incorporation of non-natural amino acids at positions 8, 9, 11, and 12 (63, 64, 68–71). Finally, in compound JMV2012, the unmodified NT_{8-13} fragment has been dimerized and cyclized (72). An advantage of the approach described here is that ANG2002 maintains the full-length sequence of NT, albeit conjugated to a single An2 molecule. More importantly, the doses used for ANG2002 were 20- to 100-fold lower than those used to test the chemically modified NT_{8-13} analogs. This advantage is probably due in part to the active diffusion of ANG2002 through the BBB, and in part to the increased plasma stability of ANG2002. In contrast to other NT analogs, the ability of ANG2002 to induce CNS efficacy at low doses may reduce adverse effects related to high exposure to peripheral nontarget organs. While NT-mediated effects on body temperature and blood pressure were observed, these effects occurred at higher doses than those required for efficacy. Another advantage of using lower concentrations is the opportunity to proceed to multitherapy for optimizing pain management. Cotherapies with lower concentrations of opioids and NT per se could result in additive or synergistic analgesic effects with only a fraction of the load of adverse effects.

Perhaps the most clinically relevant observation of this study was the demonstration of ANG2002-mediated relief of neuropathic and bone cancer pain, both of which are known to be refractory to traditional analgesic approaches (73–76). In both the CCI model and the bone marrow–implanted MRMT-1 breast cancer cell model, ANG2002 produced a rapid-onset antiallodynic effect that persisted up to 2 hours. Whether the efficacy with respect to magnitude and time course will translate to the clinic is yet to be determined. Our results with the NT receptor antagonist SR142948A and with NTS1/ NTS2 knockout mice also revealed that the analgesic effects of ANG2002 were mediated by both NTS1 and NTS2 receptors. These data reinforce previous findings demonstrating that central delivery of either NTS1 or NTS2 agonists is effective in reducing the mechanical hypersensitivity in the context of neuropathic pain (77, 78). It should also be noted that a $NT_{8–13}$ analog with a cationic non-natural amino acid at position 8, ABS212, has been shown to elicit a sustained analgesic response when administered i.p. to neuropathic rats. As with other NT analogs, this activity requires a high dose (10 mg/kg), which suggests that this drug might penetrate the BBB by passive diffusion (68). Together, these results on ANG2002-mediated relief of chronic pain are encouraging and support the potential of ANG2002 as a first-in-class NT-based chronic pain therapeutic.

As life expectancy increases, patients presenting with brain-related disorders — notably pain and neurodegenerative disorders, such as Alzheimer's or Parkinson's diseases — will grow in number. It has recently been estimated that the economic impact of brain disorders in Europe has reached €800 billion in 2010 (79). Considering the few drugs that can reach the brain parenchyma, there is a crucial need to improve CNS drug delivery by developing innovative BBB targeting technology programs. Here, we demonstrated that conjugation of An2 to a peptide rendered it brain penetrant. Moreover, after penetration of the BBB, the peptide used in this study, NT, maintained its biological activity in a battery of pain models. These results demonstrate the potential of this drug development platform for neurotherapeutics with enhanced brain penetration.

Methods

ANG2002 synthesis and conjugation

Native NT (pELYENKPRRPYIL-OH) and An2-Cys (TFFYGGSRGKRN-NFKTEEYC-NH2) were prepared by solid-phase peptide synthesis on a Symphony peptide synthesizer (Protein Technologies Inc.) using standard Fmoc chemistry with commercially available Fmoc amino acids (Chem-Impex International Inc.) and unnatural pyroglutamic acid (Sigma-Aldrich). Analysis of purity for each peptide was performed by ACQUITY UPLC (Waters Corp.) on a BEH Phenyl column (2.1 mm × 50 mm, 1.7 μm particle size; Waters) at a flow rate of 0.5 ml/min and a constant temperature of 23°C. The mobile phase consisted of a mixture of water (with 0.05% formic acid) and acetonitrile (ACN; with 0.05% formic acid). Chromatographic conditions used for analysis were as follows: isocratic (0.0 to 0.40 minutes, 98:2 water/ACN), linear gradient (until 1.2 minutes, 72:28 water/ACN), linear gradient (until 2.20 minutes, 30:70 water/ACN), linear gradient (until 2.40 minutes, 10:90 water/ACN), isocratic (until 3.00 minutes, 90:10 water/ACN), and re-equilibration (until 3.20 minutes, 98:2 water/ACN). Detection was performed at a wavelength of 229 nm, and data acquisition and processing were done using the Compass suite of instrument control and data processing software (Bruker Daltonik). Peptide identity was confirmed on a micrOTOF ESI-TOF mass spec-

trometer (Bruker Daltonik) with m/z ratios for the purified peptides of 1,672.92 Da for NT ($C_{78}H_{121}N_{21}O_{20}$) and 2,403.63 Da for An2-Cys ($C_{107}H_{155}N_{31}O_{31}S$). The conjugate ANG2002 was subsequently synthesized in PBS by a 2-step ligation method at room temperature (RT), monitored by RP-UPLC. The first conjugation step was performed in 4× PBS (pH 7.2) buffer, while the second step was in 4× PBS (pH 5.1). In the first step, a sulfo-EMCS (Molecular Biosciences Inc.) was used to incorporate a maleimidyl linker site, specifically at lysine 6 of NT, resulting in [Lys(MHA)6]NT. In the second step, conjugation with the C-terminal Cys-modified An2 peptide was performed. Both reactions were stopped by the addition of 20% acetic acid. Purification was performed on a preparative HPLC column.

LRP1-dependent binding and uptake of An2 and ANG2002

PEA-13 mouse embryonic fibroblasts (LRP1 deficient) and MEF-1 cells (WT with respect to LRP1 expression) were obtained from the American Type Culture Collection and cultured as previously described (80). $α_2M$ was purified from human plasma, as described previously (81). Activated $α_2M$ was converted into the LRP1-recognized conformation by reaction with methylamine (82) and radiolabeled with Na^{125}I, as previously described (83). For binding studies, cells were washed extensively with binding buffer (EBSS containing 25 mM HEPES and 0.1% BSA, pH 7.4) and equilibrated in binding buffer at 4°C. Cells were incubated with 0.1 nM $α_2M$-MA and increasing concentrations of unlabeled An2 in binding buffer for 4 hours. Wells were then washed 3 times with binding buffer, followed by 3 additional washes using the same medium but without BSA. Cells were lysed in 0.1 M NaOH and 1.0% SDS, and cell-associated radioactivity was determined in a gamma counter.

For fluorescent labeling, a cysteine (Bachem) was added to the C-terminal or N-terminal end of the An2 peptide to provide a sulfhydryl group for ligation of fluorochrome. Peptide labeling with the fluorochrome was performed by conjugation of Cys-containing An2 with a 2-fold molar excess of Alexa Fluor 488–C5-maleimide (Invitrogen) or 1.05-fold molar excess of β-mercaptoethanol (for probe alone; performed to stabilize the maleimide group). Conjugations were performed in the dark in PBS/DMSO buffer for 1 hour at RT under agitation. All products were purified by semipreparative high-pressure liquid chromatography on a Superdex peptide column (GE Healthcare) using an AKTAexplorer instrument. Purified product (≥95% purity) was aliquoted into separate vials, ACN was evaporated by RotaVac, and the final samples were lyophilized and frozen at –20°C under argon until further use. On the day of the experiment, each vial was resuspended in DMSO and analyzed by HPLC for quantification and to verify the integrity of all the fluorescent molecules. Each conjugation and purification step was followed by MS analysis.

To measure uptake of An2, flow cytometry studies were performed. MEF-1 and PEA-13 cells were plated at a density of $1.5 × 10^5$ cells/well and cultured overnight in 12-well plates. The culture media was then discarded, and cell monolayers were washed with PBS containing 2 mM EDTA and 0.5% BSA adjusted to pH 7.4 at 37°C, then incubated for 30 minutes at 37°C with Alexa Fluor 488–labeled An2 in Ringer/HEPES buffer (137 mM NaCl, 5.36 mM KCl, 0.4 mM Na_2HPO_4, 0.8 mM $MgCl_2$, 20 mM HEPES adjusted to pH 7.4). After incubation, cells were washed again with cold buffer and incubated with 0.5% trypsin to remove cell surface–associated fluorophore. Flow cytometry was then performed using a FACS Calibur flow cytometer with CellQuestPro software (BD Biosciences). At least 10,000 gated events per sample were analyzed. Uptake of fluorescent An2 was estimated by subtracting the background of the fluorescent probe.

CCR-2 and CCR-4 are responsible for binding more than 40 LRP1 ligands (37). We expressed CCR-2 and CCR-4 as Fc-fusion proteins, as previously described (38). In brief, CCR-2 and CCR-4 were amplified by PCR

and cloned into pFuse-rFC2 (Invivogen). CCR-2 and CCR-4 were expressed in CHO-K1 cells and purified from conditioned medium using protein A–agarose (GE Healthcare BioSciences Corp.).

In binding experiments, equimolar concentrations of CCR-2 (10 μg), CCR-4 (10 μg), or free Fc (2.5 μg) were incubated with 5 nM ^{125}I-labeled An2 in the presence or absence of 0.5 μM of the antagonist RAP (Oxford Biomedical Research), in PBS (pH 7.4) with 0.1% BSA at RT for 1 hour. Experiments were performed in triplicate. RAP is a LRP1 ligand and known competitor of An2 transcytosis across the BBB (12). The Fc-fusion proteins were affinity-precipitated with protein A–sepharose. Protein A–associated radioactivity was determined in a γ counter. Binding was expressed relative to the amount observed with [^{125}I]-An2 and free Fc. In some experiments, ^{125}I-labeled An2 was incubated with CCR-4 in the presence of 500 μM unlabeled An2 or ANG2002.

ANG2002 binding and signaling
Binding assays. Binding was carried out on freshly prepared membrane homogenates from CHO-K1 cells stably expressing the human NTS1 receptor (ES-690-C; Perkin Elmer) or on 1321N1 human astrocytoma cells stably expressing the human NTS2 receptor (ES-691-C; Perkin Elmer). Cell membranes (50 μg) were incubated with 0.2 nM [^{125}I]-Tyr^3-NT (2,200 Ci/mmol; Perkin Elmer) and increasing concentrations of NT (Bachem) or ANG2002 (from 10^{-11} to 10^{-5} M). Nonspecific radioligand binding was defined using untransfected cells. Radioactivity was counted in a γ counter. Curve fitting was performed using Graphpad Prism software to derive IC_{50} values, interpreted as the unlabeled ligand concentration inhibiting 50% of [^{125}I]-NT–specific binding.

BRET measurement. For the BRET–β-arrestin2 recruitment assay (84), the fusion vectors pIREShygro3-GFP10 and β-arrestin2–RlucII were provided by M. Bouvier (Université de Montréal, Montréal, Quebec, Canada). Using the InFusion advantage PCR cloning kit (Clontech Laboratories), the NTS1-GFP10 construct was prepared in the pIREShygro3 vector from the amplified cDNA of the gene encoding human NTS1, without a stop codon and onto which GFP10 was added to the C terminus. HEK 293T cells were grown in high-glucose DMEM supplemented with 10% FBS (Wisent). Transient expression of recombinant proteins was then performed by transfecting cells with polyethylenimine in 100-mm dishes seeded with 3×10^6 cells. 48 hours after transfection, cells coexpressing β-arrestin2–RlucII and NTS1-GFP10 were washed once with HBSS, gently detached by pipetting, and dispensed at a density of 6×10^4 cells/well into 96-well half-area white plates (Perkin Elmer). NT or ANG2002 (10^{-11} to 10^{-5} M) were added for 20 minutes, then completed with coelenterazine-400A to a final concentration of 5 μM (Goldbio). The BRET2 filters were set to monitor the 515 nm/400 nm emission ratio on the M1000 plate reader (Tecan).

To monitor direct G protein activation, we used the biosensors $G_{\alpha q}$-121-RlucII, $G_{\beta 1}$, and GFP10-$G_{\gamma 1}$ (85); $G_{\alpha o A}$-99-RlucII, $G_{\beta 1}$, and GFP10-$G_{\gamma 1}$ (86); or G_{13}-RlucII, $G_{\beta 1}$, and GFP10-$G_{\gamma 1}$. Biosensors were cotransfected with human NTS1 in HEK 293T cells using the same protocol as described for β-arrestin2 recruitment assay. 48 hours after transfection, cells were incubated with various concentrations of NT or ANG2002 (10^{-11} to 10^{-5} M) for 10 minutes and then completed with coelenterazine-400A. EC_{50} values were calculated from 3 independent experiments, each performed at least in triplicate.

Measurement of ERK1/2 activation. ERK1/2 phosphorylation in 1321N1 human astrocytoma cells stably expressing human NTS2 was monitored with an AlphaScreen SureFire pERK1/2 (Thr202/Tyr204) assay kit (Perkin Elmer), as previously described (87). Cells were seeded in 96-well plates and 24 hours later were serum-starved overnight in DMEM without glutamine and phenol red. Cells were then stimulated for 60 minutes with 1 μM NT or ANG2002. Cells were lysed with 25 μl of 5× lysis buffer and incubated on ice for 10 minutes on a plate shaker prior to being frozen

overnight at –20°C. 5 μl of the lysate was used for analysis. Readings were performed on a Perkin Elmer EnSpire 2300 Multilabel Plate Reader.

Animals
Adult male Crl:CD-1 or C57BL/6 mice (25–30 g; 14-hour light/10-hour dark cycle) and adult male Sprague-Dawley or Wistar rats (200–225 g; 12-hour light/12-hour dark cycle; Charles River Laboratories) were allowed ad libitum access to food and water. Rodents were acclimatized for 4 days to the animal facility and for 2 days to manipulations and devices prior to behavioral studies, which were performed in a quiet room by the same experimenter between 8:00 AM and 12:00 PM.

In situ brain perfusion
Iodination of ANG2002. Peptides were radiolabeled with standard procedures using a ratio of 2 iodo-beads per iodination (Iodo-beads Kit; Thermo Scientific Pierce Protein Research Products) (7). Briefly, beads were washed twice with 1 ml PBS on a Whatman filter and resuspended in 60 μl PBS (pH 6.5). [^{125}I]-Na (1 mCi) was added to the bead suspension for 5 minutes at RT. Iodination was initiated by the addition of 250 μg ANG2002 or NT (100–150 μl) diluted in 0.1 M PBS (pH 6.5). After incubation for 10 minutes at RT, iodo-beads were removed, and the supernatant was applied to a C18 column and purified by HPLC to remove free iodine. After iodination, radiolabeled products were reanalyzed by HPLC, showing >95% incorporation of radioactivity into ANG2002.

ANG2002 brain uptake. Transcytosis of [^{125}I]-ANG2002 and [^{125}I]-NT into the brains of adult male Crl:CD-1 mice was measured using an in situ brain perfusion method (88). [^{14}C]-inulin, which does not cross the BBB, was used as a physical integrity control. To carry out the perfusion protocol, the right common carotid artery of mice anesthetized with ketamine/xylazine (140:8 mg/kg i.p.) was exposed and ligatured at the level of the bifurcation of the common carotid artery, rostral to the occipital artery. The common carotid artery was then catheterized rostrally with polyethylene tubing filled with heparin (25 U/ml) mounted on a 26-gauge needle. Radiolabeled molecules were solubilized in a Krebs/bicarbonate buffer (128 mM NaCl, 24 mM $NaHCO_3$, 4.2 mM KCl, 2.4 mM NaH_2PO_4, 1.5 mM $CaCl_2$, 0.9 mM $MgCl_2$, and 9 mM D-glucose; gassed with 95% O_2 and 5% CO_2, pH 7.4, 37°C) and loaded on the infusion pump connected to the catheter (Harvard pump PHD 2000; Harvard Apparatus). Prior to the perfusion, heart ventricles were severed to eliminate the contralateral blood flow contribution. Radiolabeled test molecules were administered by carotid artery perfusion for 2 minutes at a flow rate of 2.5 ml/min, followed by a 30-second Krebs buffer washout of plasma-associated radiolabeled peptides. Mice were then decapitated to terminate perfusion, and the right hemisphere was quickly isolated on ice and subjected to further purification by capillary depletion. For capillary depletion, the mouse brain was homogenized on ice in Ringer's HEPES buffer with 0.1% BSA in a glass homogenizer. Brain homogenate was then mixed thoroughly with 35% Dextran 70 (50:50) and centrifuged at 5,400 g for 10 minutes at 4°C. The supernatant (brain parenchyma) and the pellet (capillaries) were carefully separated. Aliquots of homogenates, supernatants, pellets, and perfusates were collected at every step for determining tracer concentration for calculation of the apparent V_d.

Detection of intact [^{125}I]-ANG2002 in mouse brain homogenate. In situ brain perfusion was performed with [^{125}I]-ANG2002 as described above. Perfusion was performed for 5 minutes at 1 μM followed by a 30-second washout with Krebs buffer. At the end of the perfusion, brains were rapidly removed from the skull and the perfused (right) hemispheres were processed for ANG2002 extraction. Tissues were kept in cold homogenization buffer (0.1 M Tris-HCl, pH 5.0; 50 mM sucrose; 10× protease inhibitor cocktail) until processing. For ANG2002 extraction, brains were mechanically homogenized in ice buffer using a polytron. Cold ACN (100% with 0.05% trifluoroacetic acid [TFA]) was

added to brain homogenates to reach a final 65% ACN concentration. The mixture was stirred on a rotating mixer for 10 minutes in a cold room and then centrifuged (5,500 g for 20 minutes at 4°C). The supernatants obtained were then collected, frozen at –80°C, and vacuum-dried in a lyophilizer. Dehydrated samples were then reconstituted in mobile phase (65:35 ACN/water with 0.05% TFA). The reconstituted samples were injected onto the HPLC at a flow rate of 1 ml/min to separate and analyze the constituents. An Agilent HPLC system (1050 Series) with UV detection, along with a degasser (DGU-14A; Shimadzu), was used to study the purity of the ANG2002 radiotracer used for in situ brain perfusion and also to study the integrity of the tracer in brain tissue after perfusion. A reverse phase C-18 column (Zorbax Rx-C18, 5 μm, 4.6 mm × 150 mm) was used for analysis. The mobile phase consisted of a gradient system with water (mobile phase A) and ACN (mobile phase B), both with 0.05% TFA. The system was started at a flow rate of 1 ml/min with 2% B and held for 6 minutes. The system was ramped to 10% B from 6.01 to 11 minutes, 20% B from 11.01 to 14.0 minutes, 65% B from 20.50 to 22 minutes, 80% B from 22.10 to 24 minutes, and then brought back to 2% B from 25.00 to 32.00 minutes. Eluent samples were collected every 0.5 minutes into glass test tubes and counted for radioactivity in a γ counter.

Plasma stability of NT and ANG2002. Plasma from rat or mouse was obtained from blood after centrifugation at 16,060 g for 5 minutes at 4°C. Incubation of 27 μl rat or mouse plasma with 6 μl of a solution of 1 mM NT or ANG2002 was done at 37°C for 5 minutes over a 7-hour period. The reaction was stopped by adding 70 μl ACN. After vortexing and centrifugation at 16,060 g for 20 minutes at 4°C, the supernatant was analyzed by HPLC-MS at λ of 223 nm (Waters 2695 with ACE C_{18} column 2.0 mm × 100 mm, 2.7 μm spherical particle size and Electrospray micromass ZQ-2000 from Waters) to determine the molecular weights of the cleaved fragments.

Behavioral pain models

Acute pain models. Antinociception was assessed using different pain modalities, including hot-plate, heat radiant tail-flick, and tail immersion tests. In the hot-plate assay, male CD1 mice (25–30 g) were placed onto a metal plate heated at 54°C surrounded by a Plexiglas cylinder (13 cm × 19 cm). Baseline readings were done for each mouse immediately prior to drug injection. Animal latency to the first foot-lick was recorded (maximum 30 seconds, to prevent tissue damage). In the radiant tail-flick test, the time in seconds required to elicit a tail-flick response induced by focused radiant heat source was measured. CD1 mice manifesting an average latency of approximately 6.5–8 seconds in tail-flick response were selected and used for further testing (cutoff, 15 seconds). For the tail immersion assay performed on WT, NTS1-knockout, and NTS2-knockout C57BL/6 mice, testing involved measuring the latency for the mouse to withdraw its tail from a water bath maintained at 55°C (cutoff, 10 seconds). Subsequently, vehicle, ANG2002 (5, 10, and 20 mg/kg), and NT (8 mg/kg) were injected i.v. into the tail vein. Buprenorphine (1 mg/kg s.c.) and morphine (5 mg/kg i.p.) were used as reference drugs. Thermal threshold latencies were determined for up to 2 hours after drug injection. 8–10 mice were studied per group. Hot-plate and tail-flick latencies were used to determine MPE, calculated as (test latency – baseline latency)/(cutoff – baseline latency) and expressed as a percentage.

Persistent pain model. Antinociception was assessed using the formalin test as a model of persistent pain. For this purpose, male Sprague-Dawley rats were placed for a 60-minute habituation period in the experimentation room. Thereafter, the rats received a 50 μl s.c. injection of diluted 2% formaldehyde (i.e., 5% formalin; Fisher Scientific) into the plantar surface of the right hind paw. Subsequently, the rats were placed in clear plastic chambers (40 cm × 30 cm × 30 cm) positioned over a mirror angled at 45° in order to allow an unobstructed view of the paws, and their behaviors were scored for the next 60 minutes. An intraplantar injection of formalin produced the biphasic nociceptive response typical of this tonic pain model (42). The 2 distinct phases

of spontaneous pain behaviors that occur in rodents are proposed to reflect a direct effect of formalin on sensory receptors (phase I) and a longer-lasting pain due to inflammation and central sensitization (phase II). These 2 phases are separated by a period of quiescence, the interphase, which is characterized by active inhibition of the formalin-induced nociceptive behaviors.

Nocifensive behaviors were first assessed using a weighted score method, as described previously (89, 90). After injection of formalin into the right hind paw, the experimenter measured the time spent in each of 4 behavioral categories: 0, injected paw is comparable to contralateral paw; 1, injected paw has little or no weight placed on it; 2, injected paw is elevated, not in contact with any surface; 3, injected paw is licked, bitten, or flinched. The behaviors believed to represent higher levels of pain intensity were given higher weighted scores. The weighted average pain intensity score (ranging 0–3) was then calculated by multiplying the time spent in each category by the category weight, summing these products, and dividing by the total time in a given time interval. For a 180-second block, the pain score would thus be calculated as $(1T1 + 2T2 + 3T3)/180$, in which $T1$, $T2$, and $T3$ represent duration (in seconds) spent in behavioral categories 1, 2 and 3, respectively. Phase I and II values were calculated between 0–9 and 21–60 minutes, respectively. Alternatively, formalin-induced pain-related behaviors were quantified by monitoring the cumulative time spent in behavioral category 3 (flinching/licking/biting) during both acute (phase I) and inflammatory (phase II) phases (42). This representation of the data allowed us to determine whether the differences in pain responses after drug injection occurred at the spinal or supraspinal levels (43). Antinociceptive ED_{50} values for both phases of the formalin test were calculated from the dose-response curves generated for ANG2002 (dose ranging 0.005–5 mg/kg).

Neuropathic pain model. After baseline measurements, adult Sprague-Dawley rats underwent a surgical procedure to induce a chronic neuropathic pain state. Animals were randomly allocated to 1 of 2 surgical groups: neuropathic or sham. Neuropathic pain was induced through CCI of the sciatic nerve, as previously described by Bennett (91), with a modification in the suture used (5-0 Prolene; Ethicon Inc.) in order to minimize suture-induced inflammation. Briefly, under isoflurane anesthesia (induction at 5%, maintenance at 2.5%; Abbott Laboratories), the left sciatic nerve was loosely ligatured with 4 sutures distanced 1 mm upstream of the tibial, sural, and common peroneal nerve trifurcation. This left side was defined as the operated-ipsilateral limb, while the nonoperated leg (right) represented the contralateral side. Sham-operated rats received the same surgical procedure, except that the sciatic nerve was not ligated. Rats were housed individually for 24 hours to recover from the surgery before being housed at 4 per cage.

Bone cancer pain model. Surgical implantation of mammary carcinoma cells in the femur was performed according to Doré-Savard et al. (44, 45). Briefly, the rat right hind paw was shaved and disinfected, and a minimal skin incision (8–10 mm) was made to expose the quadriceps femoris. The vastus lateralis was incised (5–8 mm in length) to expose the femoral epicondyl, while the patellar ligament remained untouched. A small and superficial cavity (1 mm in depth) was then burred between the medial epicondyl and the adductor tubercle using a 0.8 A stereotaxic drill connected to a 1.75 mm carbide steel burr. A 25-gauge needle was next inserted at a 45° angle in that cavity to reach the intramedullar canal of the femur. The needle was substituted with a blunt-end 25-gauge needle connected to a 50-μl Hamilton syringe containing 20 μl of the mammary rat metastasis tumor (MRMT-1) cancer cell suspension (30,000 cells). The syringe was left in place for 1 minute to permit cell dispersion in the bone marrow. The needle was then removed, and the cavity was sealed with dental amalgam and polymerized with a curing light. The muscle, conjunctive tissue, and skin were closed with sutures. The impact of surgery was minimized by implantation at this anatomical site, which reduces the chances of patellar

ligament or joint damage. Sham-operated animals received the complete surgical procedure except for the implantation of mammary cells, which was replaced by vehicle injection (20 μl HBSS).

Nociceptive behavioral testing. For both chronic pain models (i.e., neuropathic and bone cancer pain), pain-related behavioral parameters were examined at day 0 (presurgical baseline) and for 21 or 18 days after injury for neuropathic or cancer-bearing animals, respectively. On the test day, rats were given ANG2002 (0.05 mg/kg i.v.), and the analgesic effect was monitored at 0, 45, 75, and 120 minutes after injection. Mechanical allodynia (e.g., pain produced by a non-noxious stimulus) was used as outcome measures of neuropathic pain development and as an indicator of analgesic efficacy of drug. To determine the presence of mechanical allodynia, rats were placed into enclosures on an elevated wire mesh floor. A dynamic plantar aesthesiometer (Ugo Basile), consisting of a metal probe (0.5 mm diameter), was directed against the hind paw pad and an upward force was exerted (3.33 g/s). PWT (i.e., the force required to elicit a withdrawal response) was measured in grams and automatically registered when the paw was withdrawn or the preset cutoff was reached (50 g). 5 values were taken alternately on both ipsilateral (operated side) and contralateral hind paws at 15-second intervals. Rats were acclimatized to the enclosures for 2 days prior to testing. Antiallodynia was determined using the area under the curve (AUC) for the 2-hour period, calculated as (post-drug latency – pre-drug latency)/ (sham latency – pre-drug latency) and expressed as a percentage (i.e., 0%, no antiallodynic effect of the compound; 100%, complete relief of mechanical hypersensitivity). The AUC was calculated over the 2-hour analgesic drug pharmacokinetic to determine whether the cumulative antiallodynic effect was significantly sustained. The trapezoid rule from the Graphpad analysis package was used (Graphpad Prism version 5.d).

Measurement of physiological variables

Core body temperature. Core body temperatures were measured using a thermistor probe inserted into the rectum of adult Sprague-Dawley rats. Temperatures were determined immediately before (baseline) and at different time points up to 6 hours after i.v. injection of vehicle or ANG2002 (0.05 or 5 mg/kg).

Blood pressure. Blood pressure parameters — systolic, diastolic, and mean blood pressure as well as heart rate — were recorded over 60 minutes using a noninvasive Coda monitor (Kent Scientific) linked to a Biopac MP150 data acquisition system with AcqKnowledge software (Biopac systems Inc.). MAP measurements were performed after administration of vehicle, ANG2002 (0.05–5 mg/kg), or NT (2 mg/kg).

Open-field test. Spontaneous locomotor activities and exploratory behaviors were evaluated 30 minutes after injection of ANG2002 at the effective analgesic dose (0.05 mg/kg i.v.). Rat were always placed facing the same direction, in the upper-left corner of an open-field testing apparatus (40 cm × 40 cm × 40 cm Plexiglas enclosure). Rat displacements were all recorded for 5 minutes with a digital camera placed directly over the apparatus. The testing began as soon as the animal was placed in the open field. The camera was attached to a computer running "Any-Maze Video Tracking System" program (Stoelting Co.), which tracked the animal and recorded its trajectory in the enclosure. Parameters analyzed were total distance traveled during the test period, mean speed, and mobile time.

Rotarod test. Motor balance and coordination were evaluated using a Rotarod (60 mm diameter, 95 mm long; IITC). Rats were acclimated on the Rotarod at 10 rpm for 2 minutes 2 days before testing. Rats were placed on the Rotarod at 4 rpm, which was gradually increased to 40 rpm over 3 minutes. Each animal had 1 trial before i.v. injection and 1 at 45 minutes after injection. Time spent on the Rotarod (in s) was measured (e.g., latency to fall). Speed (in rpm) and distance (in m) at the time of falling were also measured.

Statistics

Unless otherwise indicated, data are expressed as mean ± SEM. In vitro results were compared using 2-tailed unpaired Student's t test or 1-way ANOVA with Bonferroni post-hoc test. In vivo experiments comparing 2 groups were performed using 2-tailed unpaired Student's t test; for more than 2 groups, Brown-Forsythe test was performed to verify the variance. 1-way ANOVA corrected for multiple comparisons with Dunnett or Bonferroni post-hoc test was used. Analyses that were not normally distributed were analyzed with Kruskal-Wallis nonparametric test followed by Dunn multiple-comparison test. For 2-factor comparisons, 2-way ANOVA followed by Bonferroni post-hoc test was used. Statistical analyses were performed using GraphPad Prism (version 6.0c; GraphPad Software Inc.). A P value less than 0.05 was considered significant.

Study approval

Animal-related procedures were approved by the Ethical Committee for Animal Care and Experimentation of the Université de Sherbrooke and of the Université du Québec à Montréal and were in accordance with policies and directives of the Canadian Council on Animal Care.

Address correspondence to: Philippe Sarret, Department of Physiology and Biophysics, Faculty of Medicine and Health Sciences, Université de Sherbrooke, 3001, 12th Avenue North, Sherbrooke, Quebec J1H 5N4, Canada. Phone: 819.820.6868, ext. 12554; Fax: 819.820.6887; E-mail: Philippe.Sarret@USherbrooke.ca.

1. Daneman R. The blood-brain barrier in health and disease. *Ann Neurol.* 2012;72(5):648–672.
2. Cecchelli R, et al. Modelling of the blood-brain barrier in drug discovery and development. *Nat Rev Drug Discov.* 2007;6(8):650–661.
3. Pardridge WM. Blood-brain barrier delivery. *Drug Discov Today.* 2007;12(1–2):54–61.
4. Pardridge WM. The blood-brain barrier: bottleneck in brain drug development. *NeuroRx.* 2005;2(1):3–14.
5. Pardridge WM. Drug transport across the blood-brain barrier. *J Cereb Blood Flow Metab.* 2012; 32(11):1959–1972.
6. Gabathuler R. Approaches to transport therapeutic drugs across the blood-brain barrier to treat brain diseases. *Neurobiol Dis.* 2010;37(1):48–57.
7. Demeule M, et al. Identification and design of peptides as a new drug delivery system for the brain. *J Pharmacol Exp Ther.* 2008;324(3):1064–1072.
8. Mahley RW, Huang Y. Atherogenic remnant lipoproteins: role for proteoglycans in trapping, transferring, and internalizing. *J Clin Invest.* 2007; 117(1):94–98.
9. Strickland DK, Ashcom JD, Williams S, Burgess WH, Migliorini M, Argraves WS. Sequence identity between the alpha 2-macroglobulin receptor and low density lipoprotein receptor-related protein suggests that this molecule is a multifunctional receptor. *J Biol Chem.* 1990;265(29):17401–17404.
10. Lillis AP, Van Duyn LB, Murphy-Ullrich JE, Strickland DK. LDL receptor-related protein 1: unique

technical advance

tissue-specific functions revealed by selective gene knockout studies. *Physiol Rev*. 2008;88(3):887–918.

11. Bertrand Y, et al. Transport characteristics of a novel peptide platform for CNS therapeutics. *J Cell Mol Med*. 2010;14(12):2827–2839.

12. Demeule M, et al. Involvement of the low-density lipoprotein receptor-related protein in the transcytosis of the brain delivery vector angiopep-2. *J Neurochem*. 2008;106(4):1534–1544.

13. Che C, et al. New Angiopep-modified doxorubicin (ANG1007) and etoposide (ANG1009) chemotherapeutics with increased brain penetration. *J Med Chem*. 2010;53(7):2814–2824.

14. Regina A, et al. Antitumour activity of ANG1005, a conjugate between paclitaxel and the new brain delivery vector Angiopep-2. *Br J Pharmacol*. 2008; 155(2):185–197.

15. Thomas FC, et al. Uptake of ANG1005, a novel paclitaxel derivative, through the blood-brain barrier into brain and experimental brain metastases of breast cancer. *Pharm Res*. 2009;26(11):2486–2494.

16. Bertrand Y, et al. Influence of glioma tumour microenvironment on the transport of ANG1005 via low-density lipoprotein receptor-related protein 1. *Br J Cancer*. 2011;105(11):1697–1707.

17. Kurzrock R, et al. Safety, pharmacokinetics, and activity of GRN1005, a novel conjugate of angiopep-2, a peptide facilitating brain penetration, and paclitaxel, in patients with advanced solid tumors. *Mol Cancer Ther*. 2012;11(2):308–316.

18. Drappatz J, et al. Phase I study of GRN1005 in recurrent malignant glioma. *Clin Cancer Res*. 2013; 19(6):1567–1576.

19. Kissin I. The development of new analgesics over the past 50 years: a lack of real breakthrough drugs. *Anesth Analg*. 2010;110(3):780–789.

20. Woolf CJ. Overcoming obstacles to developing new analgesics. *Nat Med*. 2010;16(11):1241–1247.

21. Gupta A, Mehdi A, Duwell M, Sinha A. Evidence-based review of the pharmacoeconomics related to the management of chronic nonmalignant pain. *J Pain Palliat Care Pharmacother*. 2010;24(2):152–156.

22. Boules M, Li Z, Smith K, Fredrickson P, Richelson E. Diverse roles of neurotensin agonists in the central nervous system. *Front Endocrinol (Lausanne)*. 2013; 4:36.

23. Dobner PR. Neurotensin and pain modulation. *Peptides*. 2006;27(10):2405–2414.

24. Kleczkowska P, Lipkowski AW. Neurotensin and neurotensin receptors: characteristic, structure-activity relationship and pain modulation — a review. *Eur J Pharmacol*. 2013;716(1–3):54–60.

25. Sarret P, Beaudet A. Neurotensin receptors in the central nervous system. *Handbook of Chemical Neuroanatomy*. Vol. 20. Peptide Receptors, Part II. Amsterdam, the Netherlands: Elsevier; 2003:323–400.

26. al-Rodhan NR, et al. Structure-antinociceptive activity of neurotensin and some novel analogues in the periaqueductal gray region of the brainstem. *Brain Res*. 1991;557(1–2):227–235.

27. Clineschmidt BV, McGuffin JC, Bunting PB. Neurotensin: antinocisponsive action in rodents. *Eur J Pharmacol*. 1979;54(1–2):129–139.

28. Nemeroff CB, et al. Alterations in nociception and body temperature after intracisternal administration of neurotensin, beta-endorphin, other endogenous peptides, and morphine. *Proc Natl Acad Sci U S A*. 1979;76(10):5368–5371.

29. Osbahr AJ, et al. Neurotensin-induced antinociception in mice: antagonism by thyrotropin-releasing hormone. *J Pharmacol Exp Ther*. 1981;217(3):645–651.

30. Roussy G, et al. Altered morphine-induced analgesia in neurotensin type 1 receptor null mice. *Neuroscience*. 2010;170(4):1286–1294.

31. Boules M, Johnston H, Tozy J, Smith K, Li Z, Richelson E. Analgesic synergy of neurotensin receptor subtype 2 agonist NT79 and morphine. *Behav Pharmacol*. 2011;22(5–6):573–581.

32. Boules M, Shaw A, Liang Y, Barbut D, Richelson E. NT69L, a novel analgesic, shows synergy with morphine. *Brain Res*. 2009;1294:22–28.

33. Kleczkowska P, et al. PK20, a new opioid-neurotensin hybrid peptide that exhibits central and peripheral antinociceptive effects. *Mol Pain*. 2010;6:86.

34. Willnow TE, Herz J. Genetic deficiency in low density lipoprotein receptor-related protein confers cellular resistance to Pseudomonas exotoxin A. Evidence that this protein is required for uptake and degradation of multiple ligands. *J Cell Sci*. 1994; 107(pt 3):719–726.

35. Mikhailenko I, et al. Recognition of α 2-macroglobulin by the low density lipoprotein receptor-related protein requires the cooperation of two ligand binding cluster regions. *J Biol Chem*. 2001; 276(42):39484–39491.

36. Willnow TE, Orth K, Herz J. Molecular dissection of ligand binding sites on the low density lipoprotein receptor-related protein. *J Biol Chem*. 1994; 269(22):15827–15832.

37. Neels JG, van Den Berg BM, Lookene A, Olivecrona G, Pannekoek H, van Zonneveld AJ. The second and fourth cluster of class A cysteine-rich repeats of the low density lipoprotein receptor-related protein share ligand-binding properties. *J Biol Chem*. 1999; 274(44):31305–31311.

38. Fernandez-Castaneda A, et al. Identification of the low density lipoprotein (LDL) receptor-related protein-1 interactome in central nervous system myelin suggests a role in the clearance of necrotic cell debris. *J Biol Chem*. 2013;288(7):4538–4548.

39. Gully D, et al. Biochemical and pharmacological activities of SR 142948A, a new potent neurotensin receptor antagonist. *J Pharmacol Exp Ther*. 1997; 280(2):802–812.

40. Sarret P, Esdaile MJ, Perron A, Martinez J, Stroh T, Beaudet A. Potent spinal analgesia elicited through stimulation of NTS2 neurotensin receptors. *J Neurosci*. 2005;25(36):8188–8196.

41. Lafrance M, et al. Involvement of NTS2 receptors in stress-induced analgesia. *Neuroscience*. 2010; 166(2):639–652.

42. Tjolsen A, Berge OG, Hunskaar S, Rosland JH, Hole K. The formalin test: an evaluation of the method. *Pain*. 1992;51(1):5–17.

43. Sawynok J. The formalin test: characteristics and usefulness of the model. *Reviews in Analgesia*. 2004; 7:145–163.

44. Dore-Savard L, Beaudet N, Tremblay L, Xiao Y, Lepage M, Sarret P. A micro-imaging study linking bone cancer pain with tumor growth and bone resorption in a rat model. *Clin Exp Metastasis*. 2013; 30(2):225–236.

45. Dore-Savard L, et al. Behavioral, medical imaging and histopathological features of a new rat model of bone cancer pain. *PLoS One*. 2010;5(10):e13774.

46. Popp E, Schneider A, Vogel P, Teschendorf P, Bottiger BW. Time course of the hypothermic response to continuously administered neurotensin. *Neuropeptides*. 2007;41(5):349–354.

47. St-Gelais F, Jomphe C, Trudeau LE. The role of neurotensin in central nervous system pathophysiology: what is the evidence? *J Psychiatry Neurosci*. 2006; 31(4):229–245.

48. Gabathuler R. Blood-brain barrier transport of drugs for the treatment of brain diseases. *CNS Neurol Disord Drug Targets*. 2009;8(3):195–1204.

49. McGonigle P. Peptide therapeutics for CNS indications. *Biochem Pharmacol*. 2012;83(5):559–566.

50. Gabathuler R. Development of new peptide vectors for the transport of therapeutic across the blood-brain barrier. *Ther Deliv*. 2010;1(4):571–586.

51. Pardridge WM. Biopharmaceutical drug targeting to the brain. *J Drug Target*. 2010;18(3):157–167.

52. Sarret P, Perron A, Stroh T, Beaudet A. Immunohistochemical distribution of NTS2 neurotensin receptors in the rat central nervous system.

J Comp Neurol. 2003;461(4):520–538.

53. Moyse E, et al. Distribution of neurotensin binding sites in rat brain: a light microscopic radioautographic study using monoiodo [125I]Tyr3-neurotensin. *Neuroscience*. 1987;22(2):525–536.

54. Boudin H, Pelaprat D, Rostene W, Beaudet A. Cellular distribution of neurotensin receptors in rat brain: immunohistochemical study using an anti-peptide antibody against the cloned high affinity receptor. *J Comp Neurol*. 1996;373(1):76–89.

55. Sarret P, Beaudet A, Vincent JP, Mazella J. Regional and cellular distribution of low affinity neurotensin receptor mRNA in adult and developing mouse brain. *J Comp Neurol*. 1998;394(3):344–356.

56. Alexander MJ, Leeman SE. Widespread expression in adult rat forebrain of mRNA encoding high-affinity neurotensin receptor. *J Comp Neurol*. 1998; 402(4):475–500.

57. Duvernoy H, Delon S, Vannson JL. The vascularization of the human cerebellar cortex. *Brain Res Bull*. 1983;11(4):419–480.

58. Ito S, Ohtsuki S, Terasaki T. Functional characterization of the brain-to-blood efflux clearance of human amyloid-β peptide (1-40) across the rat blood-brain barrier. *Neurosci Res*. 2006;56(3):246–252.

59. Shibata M, et al. Clearance of Alzheimer's amyloid-ss(1-40) peptide from brain by LDL receptor-related protein-1 at the blood-brain barrier. *J Clin Invest*. 2000;106(12):1489–1499.

60. Machida R, Tokumura T, Tsuchiya Y, Sasaki A, Abe K. Pharmacokinetics of novel hexapeptides with neurotensin activity in rats. *Biol Pharm Bull*. 1993;16(1):43–47.

61. Tokumura T, Tanaka T, Sasaki A, Tsuchiya Y, Abe K, Machida R. Stability of a novel hexapeptide, (Me)Arg-Lys-Pro-Trp-tert-Leu-Leu-OEt, with neurotensin activity, in aqueous solution and in the solid state. *Chem Pharm Bull (Tokyo)*. 1990; 38(11):3094–3098.

62. Sarhan S, Hitchcock JM, Grauffel CA, Wettstein JG. Comparative antipsychotic profiles of neurotensin and a related systemically active peptide agonist. *Peptides*. 1997;18(8):1223–1227.

63. Orwig KS, Lassetter MR, Hadden MK, Dix TA. Comparison of N-terminal modifications on neurotensin(8-13) analogues correlates peptide stability but not binding affinity with in vivo efficacy. *J Med Chem*. 2009;52(7):1803–1813.

64. Tyler-McMahon BM, Stewart JA, Farinas F, McCormick DJ, Richelson E. Highly potent neurotensin analog that causes hypothermia and antinociception. *Eur J Pharmacol*. 2000;390(1–2):107–111.

65. Buhler AV, Choi J, Proudfit HK, Gebhart GF. Neurotensin activation of the NTR1 on spinally-projecting serotonergic neurons in the rostral ventromedial medulla is antinociceptive. *Pain*. 2005; 114(1–2):285–294.

66. Roussy G, et al. Spinal NTS1 receptors regulate nociceptive signaling in a rat formalin tonic pain model. *J Neurochem*. 2008;105(4):1100–1114.

67. Wustrow DJ, et al. Reduced amine bond neurotensin 8-13 mimetics with potent in vivo activity. *Bioorg Med Chem Lett*. 1995;5(9):997–1002.

68. Hughes FM Jr, et al. Identification and functional characterization of a stable, centrally active derivative of the neurotensin (8-13) fragment as a potential first-in-class analgesic. *J Med Chem*. 2010;53(12):4623–4632.

69. Rossi GC, Matulonis JE, Richelson E, Barbut D, Pasternak GW. Systemically and topically active antinociceptive neurotensin compounds. *J Pharmacol Exp Ther*. 2010;334(3):1075–1079.

70. Tyler BM, et al. In vitro binding and CNS effects of novel neurotensin agonists that cross the blood-brain barrier. *Neuropharmacology*. 1999; 38(7):1027–1034.

71. Boules M, et al. NT79: A novel neurotensin analog with selective behavioral effects. *Brain Res*. 2010; 1308:35–46.

72. Bredeloux P, Cavelier F, Dubuc I, Vivet B, Costentin J, Martinez J. Synthesis and biological effects of c(Lys-Lys-Pro-Tyr-Ile-Leu-Lys-Lys-Pro-Tyr-Ile-Leu) (JMV2012), a new analogue of neurotensin that crosses the blood-brain barrier. *J Med Chem*. 2008; 51(6):1610–1616.

73. Kennedy JD. Neuropathic pain: molecular complexity underlies continuing unmet medical need. *J Med Chem*. 2007;50(11):2547–2556.

74. Xu B, Descalzi G, Ye HR, Zhuo M, Wang YW. Translational investigation and treatment of neuropathic pain. *Mol Pain*. 2012;8:15.

75. Buga S, Sarria JE. The management of pain in metastatic bone disease. *Cancer Control*. 2012; 19(2):154–166.

76. Aapro MS, Coleman RE. Bone health management in patients with breast cancer: current standards and emerging strategies. *Breast*. 2012;21(1):8–19.

77. Guillemette A, Dansereau MA, Beaudet N, Richelson E, Sarret P. Intrathecal administration of NTS1 agonists reverses nociceptive behaviors in a rat model of neuropathic pain. *Eur J Pain*. 2012; 16(4):473–484.

78. Tetreault P, et al. Spinal NTS2 receptor activation reverses signs of neuropathic pain. *FASEB J*. 2013;27(9):3741–3752.

79. Gustavsson A, et al. Cost of disorders of the brain in Europe 2010. *Eur Neuropsychopharmacol*. 2011; 21(10):718–779.

80. Weaver AM, Hussaini IM, Mazar A, Henkin J, Gonias SL. Embryonic fibroblasts that are genetically deficient in low density lipoprotein receptor-related protein demonstrate increased activity of the urokinase receptor system and accelerated migration on vitronectin. *J Biol Chem*. 1997; 272(22):14372–14379.

81. Imber MJ, Pizzo SV. Clearance and binding of two electrophoretic "fast" forms of human α 2-macroglobulin. *J Biol Chem*. 1981;256(15):8134–8139.

82. Gonias SL, Reynolds JA, Pizzo SV. Physical properties of human alpha 2-macroglobulin following reaction with methylamine and trypsin. *Biochim Biophys Acta*. 1982;705(3):306–314.

83. LaMarre J, Wolf BB, Kittler EL, Quesenberry PJ, Gonias SL. Regulation of macrophage α 2-macroglobulin receptor/low density lipoprotein receptor-related protein by lipopolysaccharide and interferon-gamma. *J Clin Invest*. 1993;91(3):1219–1224.

84. Murza A, et al. Elucidation of the structure-activity relationships of apelin: influence of unnatural amino acids on binding, signaling, and plasma stability. *Chem Med Chem*. 2012;7(2):318–325.

85. Breton B, Sauvageau E, Zhou J, Bonin H, Le Gouill C, Bouvier M. Multiplexing of multicolor bioluminescence resonance energy transfer. *Biophys J*. 2010; 99(12):4037–4046.

86. Richard-Lalonde M, et al. Conformational dynamics of Kir3.1/Kir3.2 channel activation via δ-opioid receptors. *Mol Pharmacol*. 2013;83(2):416–428.

87. Koole C, et al. Allosteric ligands of the glucagon-like peptide 1 receptor (GLP-1R) differentially modulate endogenous and exogenous peptide responses in a pathway-selective manner: implications for drug screening. *Mol Pharmacol*. 2010; 78(3):456–465.

88. Dagenais C, Rousselle C, Pollack GM, Scherrmann JM. Development of an in situ mouse brain perfusion model and its application to mdr1a P-glycoprotein-deficient mice. *J Cereb Blood Flow Metab*. 2000;20(2):381–386.

89. Dubuisson D, Dennis SG. The formalin test: a quantitative study of the analgesic effects of morphine, meperidine, and brain stem stimulation in rats and cats. *Pain*. 1977;4(2):161–174.

90. Coderre TJ, Fundytus ME, McKenna JE, Dalal S, Melzack R. The formalin test: a validation of the weighted-scores method of behavioural pain rating. *Pain*. 1993;54(1):43–50.

91. Bennett GJ, Xie YK. A peripheral mononeuropathy in rat that produces disorders of pain sensation like those seen in man. *Pain*. 1988;33(1):87–107.